UNITED STATES DEPARTMENT OF ENERGY (DOE)
Announcement of Scientific and Technical Information (STI)
(For Use By Financial Assistance Recipients and Non-M&O/M&I Contractors)

OMB CONTROL NO. 1910-1400

PART I: STI PRODUCT DESCRIPTION
(To be completed by Recipient/Contractor)

A. STI Product Identifiers
1. REPORT/PRODUCT NUMBER(s)
None
2. DOE AWARD/CONTRACT NUMBER(s)
DE-FC36-97ID13554
3. OTHER IDENTIFYING NUMBER(s)
None

B. Recipient/Contractor
Edison Welding Institute, 1250 Arthur E. Adams Drive, Columbus, OH 43221

C. STI Product Title
Development of Appropriate Spot Welding Practice for Advanced High-Strength Steels

D. Author(s)
Brian Girvin, Warren Peterson, Jerry Gould

E-mail Address(es):
Brian_Girvin@EWI.org

E. STI Product Issue Date/Date of Publication
09 17 2004
MM DD YYYY

F. STI Product Type *(Select only one)*
☒ 1. TECHNICAL REPORT
☒ *Final* ☐ *Other (specify)*
☐ 2. CONFERENCE PAPER/PROCEEDINGS
Conference Information (title, location, dates)
☐ 3. JOURNAL ARTICLE
a. TYPE: ☐ *Announcement Citation Only*
☐ *Preprint* ☐ *Postprint*
b. JOURNAL NAME
c. VOLUME ____ *d. ISSUE* ____
e. SERIAL IDENTIFIER (e.g. ISSN or CODEN)
☐ 4. OTHER, SPECIFY

G. STI Product Reporting Period
08 08 2002 Thru 09 17 2004
MM DD YYYY MM DD YYYY

H. Sponsoring DOE Program Office
Office of Industrial Technologies (OIT)(EE20)

I. Subject Categories *(list primary one first)*
32 Energy Conservation, Consumption and Utilization
Keywords: Steel

J. Description/Abstract
The purpose of this project was to evaluate the effects of common manufacturing variables on spike-tempering effectiveness. The investigation examined both dual-phase and marensitic grades of high-strength steels (HSS). Common manufacturing conditions of interest included tempering practice (quench and temper time), button size, simulated part fitup and electrode wear. All these conditions were evaluated against mechanical performance (static and dynamic tensile shear). Weld hardness was also used to examine correlations between mechanical performance and the degree of tempering.

K. Intellectual Property/Distribution Limitations
(must select at least one; if uncertain contact your Contracting Officer (CO))
☒ 1. UNLIMITED ANNOUNCEMENT *(available to U.S. and non-U.S. public; the Government assumes no liability for disclosure of such data)*
☐ 2. COPYRIGHTED MATERIAL: *Are there any restrictions based on copyright?* ☐ *Yes* ☐ *No.*
If yes, list the restrictions as contained in your award document
☐ 3. PATENTABLE MATERIAL: THERE IS PATENTABLE MATERIAL IN THE DOCUMENT. *INENTION DISCLOSURE SUBMITTED TO DOE: DOE Docket Number:* S-
(Sections are marked as restricted distribution pursuant to 35 USC 205)
☐ 4. PROTECTED DATA: ☐ CRADA ☐ *Other, specify*
Release date (required) no more than 5 years from date listed in Part I.E. above MM DD YYYY
☐ 5. SMALL BUSINESS INNOVATION RESEARCH (SBIR) DATA
Release date (required) no more than 4 years from date listed in Part I.E. above MM DD YYYY
☐ 6. SMALL BUSINESS TECHNOLOGY TRANSFER RESEARCH (STTR) DATA
Release date (required) no more than 4 years from date listed in Part I.E. above MM DD YYYY
☐ 7. OFFICE OF NUCLEAR ENERGY APPLICED TECHNOLOGY

L. Recipient/Contract Point of Contact *Contact for additional information (contact or organization name To be included in published citations and who would Receive any external questions about the content of the STI Product or the research contained herein)*
Brian Girvin
Name and/or Position
Brian_Girvin@EWI.org (614)688-5117
E-mail *Phone*
Edison Welding Institute, Columbus, OH

UNITED STATES DEPARTMENT OF ENERGY (DOE)

Announcement of Scientific and Technical Information (STI)

(For Use By Financial Assistance Recipients and Non-M&O/M&I Contractors)

OMB CONTROL NO. 1910-1400

PART II: STI PRODUCT MEDIA/FORMAT and LOCATION/TRANSMISSION

(To be completed by Recipient/Contractor)

A. Media/Format Information:

1. MEDIUM OF STI PRODUCT IS:
☒ Electronic Document ☐ Computer Medium
☐ Audiovisual Material Paper
☐ No Full-text
2. SIZE OF STI PRODUCT 46 Pages
3. SPECIFY FILE FORMAT OF ELECTRONIC DOCUMENT BEING TRANSMITTED, INDICATE:
☐ SGML ☐ HTML ☐ XML ☒ PDF Normal
☐ PDF Image ☐ TIFFG4
☐ WP-indicate Version (*5.0 or greater*) ______
Platform/operation system ______
☐ MS-indicate Version (*5.0 or greater*) ______
Platform/operation system ______
☐ Postscript ______
4. IF COMPUTER MEDIUM OR AUDIOVISUAL MATERIAL:
a. Quantity/type (*specify*) ______
b. Machine compatibility (*specify*) ______
c. Other information about product format a user needs to know: ______

B. Transmission Information:

1. STI PRODUCT IS BEING TRANSMITTED:
☒ a. Electronically via E-Link
b. Via mail or shipment to address indicated in award document (*Paper product, CD-ROM, diskettes, video cassettes, etc.)* ______
2. INFORMATION PRODUCT FILE NAME
☒ *(of transmitted electronic format)*
DOENonProp0114FinalReport.

PART III: STI PRODUCT REVIEW/RELEASE INFORMATION

(To be completed by DOE)

A. STI Product Reporting Requirements Review.

☐ 1. THIS DELIVERABLE COMPLETES ALL REQUIRED DELIVERABLES FOR THIS AWARD
☐ 2. THIS DELIVERABLE FULFILLS A TECHNICAL INFORMATION REPORTING REQUIREMENT, BUT SHOULD NOT BE DISSEMINATED BEYOND DOE.

B. Award Office Is the Source of STI Product Availability

☐ THE STI PRODUCT IS NOT AVAILABLE IN AN ELECTRONIC MEDIUM. THE AWARDING OFFICE WILL SERVE AS THE INTERIM SOURCE OF AVAILABILITY.

C. DOE Releasing Official

☐ 1. I VERIFY THAT ALL NECESSARY REVIEWS HAVE BEEN COMPLETED AS DESCRIBED IN DOE G 241.1-1A, PART II, SECTION 3.0 AND THAT THE STI PRODUCT SHOULD BE RELEASED IN ACCORDANCE WITH THE INTELLECTUAL PROPERTY/DISTRIBUTION LIMITATION ABOVE.

Release by (*name*) ______

Date ___ ___ ______
MM DD YYYY

E-Mail ______

Phone ______

AISI/DOE Technology Roadmap Program

Final Report

Development of Appropriate Spot Welding Practice for Advanced High-Strength Steels

by

Brian Girvin, Warren Peterson
and
Jerry Gould

September 2004

Work Performed under Cooperative Agreement
No. DE-FC36-97ID13554

Prepared for
U.S. Department of Energy

Prepared by
American Iron and Steel Institute
Technology Roadmap Program Office
Pittsburgh, PA 15220

DISCLAIMER

Number of pages in report: 46

DOE and DOE contractors can obtain copies of this report
from:
Office of Scientific and Technical Information,
P.O. Box 62, Oak Ridge, TN 37831.
(865) 576-8401

This report is publicly available from the Department of Commerce,

National Technical Information Service,
5285 Port Royal Road,
Springfield, VA 22161.
(703) 605-6000 (1-800-553-6847).

Report Documentation Page

Title and Subtitle:

AISI/DOE Technology Roadmap Program
TRP 0114: Development of Appropriate Spot Welding Practice for Advanced High-Strength Steels

Authors:

Warren Peterson and Brian Girvin, Principal Investigators
Jerry Gould, Investigator

Performing Organization

Resistance & Solid-State Welding
Edison Welding Institute
1250 Arthur E. Adams Drive
Columbus, OH 43221

Abstract

This program evaluated the effects of common manufacturing variables on spike-tempering effectiveness. The investigation used design-of-experiment (DOE) techniques, and examined both dual-phase and martensitic grades of high-strength steels (HSS). The specific grades chosen for this project were:

- Dual-phase (DP) 600, galvannealed (GA), 1.55 mm (DP) 600
- Dual-phase (DP) 980 (uncoated), 1.55 mm (DP) 980
- Martensitic (M) 1300, 1.55 mm (M) 1300

Common manufacturing conditions of interest included tempering practice (quench and temper time), button size, simulated part fitup (sheet angular misalignment and fitup), and electrode wear (increased electrode face diameter). All of these conditions were evaluated against mechanical performance (static and dynamic tensile shear). Weld hardness data was also used to examine correlations between mechanical performance and the degree of tempering.

Mechanical performance data was used to develop empirical models. The models were used to examine the robustness of weld strength and toughness to the selected processing conditions. This was done using standard EWI techniques. Graphical representations of robustness were then coupled with metallographic data to relate mechanical properties to the effectiveness of spike tempering.

Mechanical properties for all three materials were relatively robust to variation in tempering. Major deviations in mechical properties were caused by degradation of the weld itself. This was supported by a lack of correlation between hardness data and mechanical results. Small button sizes and large electrode face diameters (worn electrodes) produced large reductions in both static and dynamic strength levels when compared to standard production setups. Dynamic strength was further degraded by edge-located welds.

.

(RDP Standard Form, Form 298)

November 10, 2004
EWI Project No. 47819GTH

Development of Appropriate Spot Welding Practice for Advanced High-Strength Steels

Submitted to:
American Iron and Steel Institute
Pittsburgh, PA

Report
Project No. 47819GTH

on

Development of Appropriate Spot Welding Practice for Advanced High-Strength Steels

to

American Iron and Steel Institute
Pittsburgh, PA

November 10, 2004

Brian Girvin, Jerry Gould, and Warren Peterson
EWI
1250 Arthur E. Adams Drive
Columbus, OH 43221

Contents

Page

Tables

Page

Figures

Note that Appendices A, B and C include Protected Metals Initiative Data and are hereby withheld from this report in accordance with the Intellectual Property provisions of the AISI/DOE Cooperative Agreement DE-FC36-97ID13554.

Executive Summary

This program evaluated the effects of common manufacturing variables on spike-tempering effectiveness. The investigation used design-of-experiment (DOE) techniques, and examined both dual-phase and martensitic grades of high-strength steels (HSS). The specific grades chosen for this project were:

- Dual-phase (DP) 600, galvannealed (GA), 1.55 mm (DP) 600
- Dual-phase (DP) 980 (uncoated), 1.55 mm (DP) 980
- Martensitic (M) 1300, 1.55 mm (M) 1300

Common manufacturing conditions of interest included tempering practice (quench and temper time), button size, simulated part fitup (sheet angular misalignment and fitup), and electrode wear (increased electrode face diameter). All of these conditions were evaluated against mechanical performance (static and dynamic tensile shear). Weld hardness data was also used to examine correlations between mechanical performance and the degree of tempering.

Mechanical performance data was used to develop empirical models. The models were used to examine the robustness of weld strength and toughness to the selected processing conditions. This was done using standard EWI techniques. Graphical representations of robustness were then coupled with metallographic data to relate mechanical properties to the effectiveness of spike tempering.

Mechanical properties for all three materials were relatively robust to variation in tempering. Major deviations in mechical properties were caused by degradation of the weld itself. This was supported by a lack of correlation between hardness data and mechanical results. Small button sizes and large electrode face diameters (worn electrodes) produced large reductions in both static and dynamic strength levels when compared to standard production setups. Dynamic strength was further degraded by edge-located welds.

1.0 Introduction

Fuel efficiency standards promote lightweight automotive structural designs that rely on high-strength steels (HSS) to optimize weight and performance. HSS are still preferred over alternative lightweight materials due to the relative cost. Recently, a range of advanced high-strength steels (AHSS) have been introduced. These include dual-phase (DP), transformation-induced plasticity (TRIP), and martensitic grades. All of these grades appear to meet requirements for formability, but weld metal fracture associated with resistance spot welding (RSW) of these steels has been a concern. More specifically, these grades of materials are susceptible to a phenomenon known as hold time sensitivity (HTS). HTS is usually demonstrated during peel tests, where longer hold times yield interfacial failure modes.

Recent investigations have reduced HTS through in-situ tempering. These studies were conducted in order to develop acceptable welding and tempering conditions for the steel grades mentioned earlier. Results from these investigations have shown that short temper schedules, “spike-tempers,” are effective for improving weld metal fracture toughness while retaining joint strength. The effects of manufacturing conditions on the usefulness of this technique, however, are unknown.

This project examines the effect of typical manufacturing variables on the effectiveness of spike tempering. Manufacturing factors included geometric concerns (part fitup, part alignment, part gap, button size), electrode wear concerns (electrode face diameter), and tempering concerns (quench and temper time). To facilitate this work, experimental design (DOE) methodologies were employed. DOE results were used to develop empirical models that relate processing conditions to both static and dynamic mechanical properties. This was done for two grades of DP steel (DP600 and -980), and one grade of martensitic steel (M1300). The models were then used to develop graphical representations of process robustness. This was done in order to determine the relative effect of each factor on mechanical performance, as well as the robustness of spike tempering. Results were supported with metallographic observations.

2.0 Experimental Techniques

2.1 Materials and Coupon Dimensions

The steels chosen by the sponsors for this phase of the program included:

- DP600, galvannealed (GA), 1.55 mm (DP) 600
- DP980 (uncoated), 1.50 mm (DP) 980
- Martensitic (M) 1300, 1.56 mm (M) 1300

Individual chemistries are given in Table 1.

Weld coupons for the static, dynamic, and metallographic specimens measured 125 × 200 mm (5 × 8 in). Slightly longer dynamic coupons were used to accommodate a 180-degree radiused bend at one end. Peal coupons measured 38 × 125 mm (1.5 × 5 in.).

2.2 Equipment

A Newcor 200-kVA single-phase AC pedestal-type spot welder was used in this investigation. This machine used a Medar Legend controller that was set up for phase-shift control (constant voltage). Constant voltage control was used due to the relatively short duration of the temper pulse.

Welding and temper currents were measured using a Miyachi MM326 weld checker. Weld force was measured using an oil-filled Waka force gage. Weld button measurements were made with Mitutoyo knife-edge digital calipers.

2.3 Experimental Design

For this program, a 7-factor, two-level, Resolution IV fractional-factorial design was used. Factors and their associated levels were:

- Quench time (20 cycles, 40 cycles)
- Temper time (2 cycles, 4 cycles)
- Button size ($4\sqrt{t}$, $6\sqrt{t}$)
- Electrode face diameter (8 mm, 9 mm)
- Angular misalignment (perpendicular, 10-degree offset)
- Weld position (center of coupon overlap, 0.5 mm from edge)
- Fitup (good fitup, 2t gap)

Quench time levels were obtained from previous work and were verified using analytical models(1) that predicted the critical cooling rate. These results suggested that the longer (40 cycle) was necessary for complete transformation on these particular gauges of steels. Temper times were chosen from different regions of the previously developed spike-temper diagrams.(2)

The 2-cycle temper time was chosen to provide a stable, but nearly adiabatic thermal cycle across the weld region. The 4-cycle temper time, alternately, has been seen to allow some electrode cooling effects, but still be considered within the spike-temper regime.[2]

Button sizes were chosen based on several recommended practice documents, again based on the 1.55-mm sheet thickness.[3-5] Button size levels were 5.21 and 7.35 mm for the low and high levels, respectively. Electrode face sizes were also nominally taken from these documents. The low (8-mm) level of electrode face diameter was taken from the Ford BA 013-04 specification.[3] The high (9-mm) level was chosen somewhat arbitrarily, and was selected to simulate extreme electrode wear. Angular misalignment variations were defined based on previous work,[6-9] with levels planned at zero and 15 degrees. Small button diameters could not reliably be achieved at the most severe tilt condition. As a result, a 10-degree angle was incorporated in the final DOE. Weld position and fitup levels were based on previous studies[6-10] and on discussions with the sponsor.

The experimental design was of reduced resolution, and therefore had some two-factor confounding. To manage this confounding, significant two-factor interactions were ranked from 0 to 10 based on the degree of significance. Rankings were based on EWI's past experience. The individual columns in the experimental matrix were then organized to eliminate the grouping of multiple significant interactions. Interactions deemed significant were mainly those involving quench time, although some involving electrode face diameter were also identified.

2.4 Setup

In the experimental trials, a special fixture was used to support and position the coupons relative to the electrodes. The fixture also facilitated angular rotation for the misalignment condition. Male, Class 2, RWMA 6, 45-degree truncated cone-type electrodes were used for all trials. Face diameters were 8 and 9 mm, as mentioned above. Prior to use, the electrodes were aligned using a coupon wrapped in emery cloth. Parallelism was accomplished by rotating the paper and coupon between the electrodes using reduced electrode pressure. Alignment was confirmed using carbon imprints.

2.5 Screening Trials

Screening trials were conducted to help properly scale the experiment. Particularly the effort was made, through these screening trials, to minimize the occurrence of no-weld conditions in the experiment. As a first step, current range data was collected for each electrode face diameter on the 38-mm-wide samples in the optimal condition (perpendicular alignment, good fitup). This was done to reveal the required levels for the high and low button sizes. The welding practice was taken from previous phases, and involved a weld force of 5.5 kN (1200 lb), and welding times of 17 and 19 cycles, depending on the steel grade.

Once weld currents were identified for the small button size, “worst-case” welding conditions were attempted to ensure bond integrity throughout the experiment. These particular tests focused on poor angular alignment and fitup conditions. Initial angular offsets were examined at 10 and 15 degrees (using the higher strength grades of steel and with the small button size). Poor fitup conditions were simulated with 1, 2, and 3t gaps between the coupon overlap. The gaps were obtained by inserting 13-mm-wide $\times$ 125-mm-long (0.5-in.-wide $\times$ 5-in.-long) shims at the outermost edges of the overlap. To account for the edge-position welds, the shims had to be oriented the same direction as the weld fixture (perpendicular to the machine). Similar to the angular offset trials, poor fitup was examined using the higher strength steels and using the smaller button size. As a final check, these tests were duplicated using larger electrode face diameters.

Results from these trials showed that a 15-degree angular misalignment was too severe, particularly in combination with the larger (9-mm) electrode face diameter. A 3t level of poor fitup or gap was also determined to be excessive when used in combination with angular misalignment, large electrode face diameters, and small button sizes. Angular misalignments of 10 degrees and part gaps of 2t appeared to be acceptable in terms of maintaining an “in-tact” weld specimen, and were severe enough to examine variation. These two levels were eventually picked for the final DOE levels (Table 2).

2.6 Tempering Trials

Temper trials were conducted to define acceptable tempering currents (in the center of the C-curve portion of the temper map) for the steels used in these experiments. Tempering trials were carried out with the smaller 38-mm (1.5-in.) -wide coupons, and used weld surface hardness to define the degree of tempering. All samples were generated using previously defined weld schedules for the grade of steel involved. Welding was done in the flat (perpendicular) position with good fitup, and using the small electrode face diameter and small button size. Acceptable tempering currents were identified by choosing the point at which maximum softening had occurred. These levels were further confirmed by peel testing. This was done through conformation of full peel buttons. In all cases, full button pull was consistent with the hardness “dip” obtained from the range curves. Tempering currents were identified for each level of temper time planned in the DOE outlined above. No allowances were made for any of the other variables studied. Welding schedules and tempering currents are presented in Table 3.

2.7 DOE Welding Trials

For each of the DOE trials, electrode setups were conducted in a manner described in Section 2.4 above. Conditioning of the electrodes was then dependent on the material coating. For the DP600 GA material, 200 conditioning welds were done to stabilize the condition of the electrode face. Approximately 25 conditioning welds were performed with the DP980 and M1300 uncoated grades.

For each set of processing conditions in the DOE, button size was confirmed using the 38 × 125 mm (1.5 × 5 in.) peel samples. Peel specimens were done with a single weld positioned in the center of the overlap, and were always done in the flat position and with good fitup. Shunt welds were not employed on the peel samples, in order to more accurately mimic the mechanical test samples to be produced.

Despite the efforts to avoid no-weld conditions in the DOE, it was noted that during some trials involving angular misalignment, the sheets would detach at cycle completion. This was particularly true for schedules involving a short quench time in combination with a large electrode face and a small button size. In order to mitigate this issue, button size determinations for trials involving angular misalignment were no longer done in the flat position. Rather, the button size determination was done in the angled position, mimicking the conditions of the trial itself. This had the effect of essentially prorating the welding current to the angular misalignment.

Once button size was confirmed, six representative samples were made for mechanical and metallographic testing. Two of the samples were for static tensile shear tests, two were for dynamic tensile shear tests, and one was for metallographic examinations. The remaining sample was retained as a spare.

2.8 Statistical Analysis of the Data

Statistical analysis of the data was done using the standard EWI methodology. This methodology has been detailed at length elsewhere.[6-8] Essentially, the methodology consists of five steps:

1. Normalization of the response data
2. Stepwise regression analysis
3. Regression analysis/model development
4. Reverse transformation of the model
5. Preparation of robustness plots.

Normalization of the response data is a critical first step to achieving accuracy from statistical models. This is because statistical models are based on inference from comparisons of normal distributions of data. Unfortunately, most real data is not normally distributed. In this case, a range of mathematical transforms can be used to improve the normality of such data. Such transforms must be both monotonic, and continuous over the data range of interest. In this study, each set of response data was tested for normality using Minitab® 13.0 software. Normality was assessed both numerically and graphically by comparison with mean and standard-deviation results. Normality corrections (where required) were then applied using a limited range of transformation functions, and varying weighting constants in an iterative fashion. These normalization functions were then retained, and the transformed data used for subsequent analysis.

Stepwise regression analysis is essentially the process of defining the factors for inclusion in the statistical model. This, again, was done through Minitab® 13.0 software. During stepwise analysis, factors are selected progressively, based on their correlation with the (now normal) response data. Main effects and two-factor interactions are continually selected until no remaining factor has a correlation statistic above a critical value. Identified factors (main effects and two-factor interactions) are then used for the full regression analysis.

Regression analysis/model building refers to the development of a full statistical model. In this step, the factors and interactions identified by stepwise regression analysis are regressed (again in this study with Minitab® 13.0) against each response variable of interest. The resulting models contain all necessary constants and qualification statistics.

Reverse transformation of the models is the final step in the model building process. As mentioned above, the core statistical models are based on the normally transformed data, and must be back transformed to represent the raw data. These back transformations are essentially the inverse functions of the normalization functions described above. These inverse, or back-transformation functions must also be both monotonic and continuous over the response range of interest. Results from these back-transformed statistical models are then used to develop the process robustness plots described below.

Robustness plots are visual vehicle used for interpreting the results of DOE-based studies. Process robustness plots are created by first identifying some best or acceptable practice (combination of experimental factors). Then, the response characteristic is plotted as a function of each factor as it is varied from those conditions. This approach has three benefits. First, it allows relatively complicated response models (in this case, up to 7 factors) to be viewed as a series of two-dimensional projections. Second, critical (and non-critical) factors can be quickly identified. Finally, for critical process (and setup) variables, acceptable ranges of variations can be graphically identified.

2.9 Microscopy and Hardness Data

Metallographic samples were prepared by sectioning normal to the weld along the centerline. The resulting sections were then metallographically prepared using standard techniques. Etching was performed using 2% Nital. Sectioning was done along the longitudinal axis of the coupon.

Hardness traverses were done using a series of Vickers microhardness measurements (1-kg load, 15 s). The hardness traverse was done normal to the faying surface, along the central axis of the weld.

3.0 Results

3.1 Statistical Analysis

The mechanical test data (Tables 4 and 5) was analyzed using the statistical approach outlined in Section 2.8 above. Six different analyses were conducted as part of this program. This included analysis of peak loads during static testing, and absorbed energies during dynamic testing for each of the three materials. Several samples made using the DP grades detached during shipment to the mechanical test lab. For these samples, zeros were recorded in the dataset. Two of the six datasets (DP600-dynamic testing and M1300-dynamic testing) required data transformation prior to analysis in order to restore normality. Transformation equations are shown in Table 6. Once normality correction was complete, the analyses were performed in the standard fashion.

The resulting regression models generally had good correlations with the data. With the exception of the M1300 dynamic model, R^2 values were well above 80%. These regression models, along with their associated correlation factors are presented in Tables 7-12.

The resulting models were then used to create graphical representations of process robustness. In this process, the DP600 and M1300 dynamic models required back-transformation in order yield the force and energy data needed in the plots. The resulting process robustness plots are presented in Section 3.2 below.

3.2 Process Robustness Results

As described in Section 3.1 above, the regression equations derived for each response and material grade were used to develop graphical representations of process robustness. The process robustness diagrams presented here are anchored on appropriate production settings and are presented in Figures 1-6. Each factors effect on mechanical performance data is shown. The plots were created by varying each factor level individually (from low to high) based on the “anchored” conditions. The anchored conditions are as follows:

- Quench time: 40 cycles (high level)
- Temper time: 4 cycles (low level)
- Button size: 6vt (high level)
- Electrode face diameter: 8-mm (low level)
- Angular misalignment: None or perpendicular (high level)
- Weld position: Center of coupon overlap (high level)
- Fitup: No gap (high level).

Descriptions of these plots for the individual materials are given below.

3.3 DP600 Static Tensile Shear Results

The process robustness plot for the static tensile shear test results on the DP600 steel is shown in Figure 1. Static tensile shear (peak load) for the DP600 material was strongly influenced by the electrode face diameter and button size. The effect of weld position and angular alignment was notable, although not as significant. Quantitatively, the effects of the individual factors, when varied from the anchored conditions, are as follows:

- Large electrode face diameter – decrease of 54%
- Small button size – decrease of 42%
- Edge located weld – decrease of 15%
- 10-degree angular misalignment – decrease of 13%
- Short (2-cycle) temper time – increase of 2%
- Short quench time – decrease of 1.42%

Quench and temper times, as well as fitup condition had almost no effect on static performance.

3.4 DP980 Static Tensile Shear Results

The process robustness plot for the static shear tensile shear test results on the DP980 steel is shown in Figure 2. The plot is somewhat similar to that seen for the DP600 steel (Figure 1 above), and is again dominated by the effects of button size and electrode face diameter. In this case, however, weld location did not have any effect. The quantitative impact of varying each factor from the anchored conditions is as follows:

- Small button size – decrease of 48%
- Large electrode face diameter – decrease of 35%
- Short (20-cycle) quench time – increase of 20%
- 10-degree angular misalignment – increase of 17%
- Poor fitup – decrease of 10%
- Short temper – decrease of 9%
- Edge located weld – decrease of 0.5%

The effect of quench and temper time was reversed from that found on the DP600 material. The DP980 material appears to favor short quench times and long temper times. Compared to the other factors, however, these effects were minimal.

3.5 M1300 Static Tensile Shear Results

The process robustness plot for the static tensile shear results from the M1300 material is presented in Figure 3. Overall, the observed variations in static strength were small compared to the two other materials. Strengths on this plot do not fall below 16 kN. The largest effect was due to changes in button size. The quantitative impact of varying each factor from the anchored conditions is as follows:

- Small button size – decrease of 44%
- Large electrode face diameter – decrease of 18%
- Short temper – decrease of 17%
- Short quench – decrease of 14%
- Edge located weld – decrease of 2%

Angular alignment and fitup conditions did not affect the static results.

3.6 DP600 Dynamic Tensile Shear Results

The process robustness plot showing the dynamic shear energy results (energy at peak load) is presented in Figure 4. The most notable characteristic of this plot is the reduction in dynamic tensile shear energy with application of a number of factors. These included small button sizes, large electrode face diameters, and edge position of the weld. The short quench times moderately reduced impact energies, while the shorter temper times moderately improved them. The quantitative impact of varying each factor from the anchored conditions is as follows:

- Small button size – decrease of 100%
- Edge located weld – decrease of 100%
- Large electrode face diameter – decrease of 95%
- Poor fitup – increase of 76%
- 10-degree angular misalignment – increase of 40%
- Short quench time – decrease of 32%
- Short (2-cycle) temper time – increase of 16%

Of note, poor fitup appeared to greatly improve impact energies when welding this steel. Reasons for this are not clear; however, a similar effect was not seen for the other steels of this study.

3.7 DP980 Dynamic Tensile Shear Results

The process robustness plot for the dynamic shear energies for the DP980 steel is presented in Figure 5. These results generally tracked with the static tensile results presented above. With the exception of fitup, all factors appeared to influence the impact results of the DP980 steel. The quantitative impact of varying each factor from the anchored conditions is as follows:

- Edge located weld – decrease of 80%
- Small button size – decrease of 76%
- Large electrode face diameter – decrease of 27%
- Short temper – decrease of 18%
- Short (20-cycle) quench time –decrease of 5%
- 10-degree angular misalignment – increase of 2%

3.8 M1300 Dynamic Tensile Shear Results

The process robustness plot for the dynamic tensile shear results on the M1300 steel are presented in Figure 6. The dynamic tensile shear results were again dominated by the effect of button size. Edge position also had a moderate effect. The quantitative impact of varying each factor from the anchored conditions is as follows:

- Small button size – decrease of 100%
- Edge located weld – decrease of 28%
- Large electrode face diameter – decrease of 9%
- Short quench – decrease of 3%

Temper time, angular alignment, and fitup conditions had no apparent effect on dynamic performance for this material. The insensitivity to fitup conditions for this grade of material was consistent with results obtained from the static analysis.

3.9 Hardness Observations

Through-thickness hardness data was collected and is presented for each trial in Appendices A-C. These appendices includes both the hardness plot, and a micrograph of the weld nugget itself. This data was examined visually, and was correlated with mechanical results to examine similarities. Both peak and averaged hardness results were used. These correlations are described in the following sections.

3.9.1 Optimal Conditions for Tempering

Hardness traverses were not examined statistically, but were compared and contrasted against the different factor settings. From these examinations, the following factors were determined to be optimal for effective tempering:

- Quench time – 40 cycles
- Button size – small (4vt)
- Electrode face diameter – small (8 mm)
- Weld position – center of overlap

This practice was consistent for all the materials examined.

3.9.2 Correlations with Mechanical Data

In order to examine similarities between hardness and mechanical data, both averaged and peak hardness data was overlaid on average strength data (both static and dynamic). The data was plotted by trial number. Hardness data was also plotted directly as a function of strength data. Results showed that the mechanical performance data was largely insensitive to variations in weld hardness over the ranges studied. Data illustrating this is shown in Figures 7-10 for the impact data. Results from the static data, are not shown, but are similar.

3.10 Nugget Measurements from Mechanical Specimens

Nugget measurements were recorded from processed static and dynamic test specimens. Residual buttons, if present, were measured as well. This data is shown in Tables 13 and 14. In most cases, the welds failed in shear, although parent metal pull-out (a weld button) was evident on many of the trials involving edge located welds. Button pulls were more frequent on the higher strength steels compared to the DP600 material.

4.0 Discussion

4.1 Influence of Geometry

Factors which affected the geometry of the specimen clearly dominated the performance of welds made on all three grades of steels. These included the electrode face diameter, the weld position, the weld size, and the angular alignment. The most important of these attributes was the size of the weld itself. The relationship between static strengths and weld size has long been established.(11,12) In general, larger weld sizes lead to improved mechanical properties. That fact was certainly reflected here. Reducing weld size was particularly detrimental to impact performance.

Regarding AHSS, previous studies(13,14) have noted the effect of weld size on susceptibility to interfacial fracture, with subsequent reduced performance. Generally, it was suggested that three factors relate to such failures. These include a fracture sensitive (high hardness) microstructure, a preferential crack path (weld related porosity), and a disadvantageous stress state. Further, it was noted that in the extreme, any one of these factors could be related to reduced performance. In these studies, the hardness profiles suggest significant toughening of the weld microstructure, and the micrographs do not infer the presence of extensive porosity. As a result, stress state appears to be the dominant cause of performance variations. For static testing, the larger weld sizes both increase the overall bond area, and promote nugget rotation, reducing tendency for shear-type failures. Both directly affect the required load to produce failure. In addition, as suggested above, weld size also affects the stress state.

Electrode face diameter also turned out to be a critical factor. Mechanical properties associated with the DP600 material were most adversely affected by the larger face diameters, although the DP980 also showed major sensitivity. Metallographic work (see Appendices A-C) shows that welds made with small face diameters exhibit a much more consistent fusion zone at the outer regions of the weld compared to those using the larger face. The influence of increasing electrode face size on weld morphology is well documented.(15,16) As electrodes increase in size, weld nugget geometries vary from ellipsoidal to toroidal to crescent shaped. This effect is due to thermal instabilities, which result as the electrode diameter-to-sheet thickness ratio becomes excessively large. In these studies, button sizes were confirmed for each trial. This was done using the smaller (1.5-in.-wide) coupons. Additionally, this was done with no constraint (flat position, with good fitup). Test specimens, however, were made on the 5-in.-wide coupons, and clearly show a reduced degree of fusion compared to that observed on the smaller coupons. This suggests that the additional thermal constraint associated with the larger coupons has effected weld formation. The effect is particularly evident with the higher strength material grades.

The effect of weld position was consistent for all grades of material and for both mechanical measures. Edge-located welds reduced performance. Of the three materials, the DP600 suffered the greatest performance losses due to this factor. Reasons for this are most likely related to HAZ softening characteristics. The DP980 and M1300 materials both experience significant softening in the HAZ due to welding. The DP600 material, however, experiences minimal softening about the weld periphery. The effect was noted in the first two phases of this program. HAZ softening tends to make the higher strength grades fail in a ductile fashion, with initiation occurring in the softened region. This is clear from viewing button measurements taken from the failed mechanical samples. Data clearly shows that full button pull-outs were more pronounced with the higher strength grades, and that all button pulls were associated with edge-located welds. The lower strength (DP600 material), however, tended to fail in a shear mode, which was most likely caused by the minimization of a metallurgical notch.

The effect of weld position was most prominent for impact strength, but was also significant for static tensile strength. This change in sensitivity is probably related to the reduced tendency for nugget rotation during the impact tests.

The effect of angular position has been documented in separate research(6-8) and has been shown to drastically affect weld performance by promoting a deleterious stress buildup at the weld periphery. In this program, the effect was partially masked by prorating the current during the DOE trials. As a result, this factor did not appear to be as significant as the other geometric factors. In reality, the effect of angular misalignment is probably more severe than any of the other factors examined. The sensitivity of the three materials to angular misalignment paralleled the response to edge position (DP600 most sensitive, M1300 least sensitive). Reasons for this can again be related to the degree of softening about the weld periphery. The DP600 material, due to its resistance to HAZ softening, is more susceptible to stress “pileups” at the outer edges of the weld, while the M1300 can better accommodate these buildups by yielding in the softened region.

4.2 Effects of Tempering Conditions

The variation in temper times examined here minimally affected mechanical performance, particularly compared to the geometric factors. This is not surprising given that temper times were purposely chosen in the spike-tempering regime of the temper maps. In general, the preference was for the longer temper time, particularly with the higher strength materials.

Overall, hardness drops were greater when the smaller button size was employed. For the DP600 material, this is apparent from viewing Trials 2, 4, 5, and 6 (Figures A-2, A-4, A-5, and A-6, Appendix A). Trials 2 and 4 were done using the smaller button size, and clearly show an adequate degree of softening compared to maximum attainable hardness. These particular trials, however, produced substantially lower mechanical strengths. Figures 5 and 6, on the other hand, showed welding conditions involving the larger button size and clearly illustrate that substantial softening was never achieved. Nevertheless, Trials 5 and 6 produced the best mechanical properties in terms of both static and dynamic criteria. There are two possible reasons for differences in tempering response. First, the quench times may have been inadequate for the large button size. In addition, the larger weld may have provided a larger current conducting area, reducing effective current density and subsequently tempering effectiveness. Clearly, the degree of tempering appears secondary to good geometric conditions. In addition, the harder weld is inherently stronger, offering greater resistance to the shear-type failures generally observed in this study. The difference in results for small and large button sizes helps explain the relatively stable robustness of this factor in the experiment.

4.3 Process Robustness of the Spike-Tempering Approach

As detailed above, the dominant factors affecting performance were largely geometric, rather than related to the spike-tempering approach itself. For the three steels studied, actual variations in spike-tempering practice resulted in minimal variation in mechanical performance. This would suggest the spike-tempering process is quite robust, not only with respect to variations in the tempering conditions themselves, but also regarding other manufacturing variations (electrode size, electrode alignment, etc.). As described above, however, some sensitivity is masked due to the scaling of temper currents to temper time. The shape of the spike-temper diagram[(17)] clearly shows that the degree of tempering is quite sensitive to variations in time (at a fixed current) but relatively insensitive to variations in current (at a fixed time). Fortunately, the process can be precisely controlled in time (most modern controllers are accurate to 10s of μs), and must be considered robust even with the implied sensitivity from the spike-temper diagram itself.

Factors that lead to current concentrations in the weld area also affect temper response. These include fitup, button size, and potentially alignment. In these cases, the area for conduction during tempering is reduced, causing exaggerated heating during tempering at a fixed current. This, in turn, based on the current dependency indicated in the spike-temper diagram, can cause variations in the effective temper response.

Finally, factors that effect thermal response can cause variations in tempering behavior. These include, potentially, proximity to the edge, electrode size, and even alignment. In the former case, proximity to the edge reduces potential heat losses to surrounding material by the introduction of a non-conducting boundary (the edge itself). It has been demonstrated elsewhere[(18)] for the thicknesses of steel studied here, these edge losses could be as high as 40% of the heat generated in the weld. Elimination of this conductive path would have the effect of overheating the temper area, potentially resulting in re-austenization and re-formation of martensite. Conversely, excessively large electrode diameters can heat sink the weld during tempering, reducing the temper response. The opposite of this is the effect of poor alignment. In this case, the smaller implied electrode contact area reduces heat extraction during tempering, potentially increasing the tempering response.

Despite all the potential effects of geometric factors on tempering effectiveness, button morphologies from failed mechanical samples failed to show any evidence of interface-type failures. This suggests that spike tempering is quite robust to current (or current density) variations, and should be applicable to a range of manufacturing environments.

5.0 Conclusions

In this program, the robustness of the spike-tempering approach regarding a range of manufacturing conditions has been evaluated. Work as been conducted on three representative AHSS. These include DP600, DP980, and M1300 steels, all ranging from 1.5 to 1.56 mm in thickness. Factors included in the robustness analysis included quench time, temper time, button size, electrode face diameter, angular misalignment, weld position, and fitup. Work was done using DOE approaches. A 16-trial fractional-factorial experiment was conducted for each steel. Response variables for this analysis included static tensile properties and impact tensile properties. Metallographic sections along with through-thickness hardness traces were also collected for reference purposes. Results were then analyzed using regression techniques, and prepared graphically as process robustness plots. Specific conclusions from this program include:

(1) **Overall robustness of the spike-tempering approach:** Overall process robustness for the application of spike tempering was dominated by geometric effects. There was relatively less influence of actual spike-tempering variables (temper time, quench time) on joint performance.

(2) **General characteristics of hardness profiles:** All hardness profiles maintained the characteristic top hat shape, indicating uniform softening because of the spike-tempering process. This was not surprising, as temper times and currents were all selected within the spike-temper region of the overall temper curve.

(3) **Failure modes during mechanical testing:** All welds failed by either shear or button pull-out. This is a reflection of toughness improvements associated with spike tempering across the range of materials, setup conditions, and tempering conditions used in this study.

(4) **Significance of geometric factors:** Geometric factors dominated the results seen in these experiments. In particular, large weld sizes were the single strongest factor affecting weld performance. This was related to the load bearing area of the weld, as well as the reduced stress concentration factors associated with larger weld sizes. Factors, which influenced the degree of nugget rotation during testing (e.g., edge position), also affected the results, especially impact performance.

(5) **Prorating of temper current during the experimental trials:** In these studies, the temper current was prorated to temper time based on the temper map C-curve.

However, the shape of the spike-temper curves indicates considerable robustness to variations in tempering current due to typical fitup and misalignment conditions.

(6) **<u>Heat transfer and current density-related effects</u>:** Geometric (misalignments, poor fitups) and simulated electrode wear (large electrode face diameters) factors affected the conducting area for flow of the weld current and the thermal response of the weld. This necessitated some prorating of weld current values in order to preserve adequate button sizes. Again, the shape of the spike-temper curves indicates considerable robustness to such variations in current.

(7) **<u>Relative sensitivity of the materials tested</u>:** All materials showed the same general trends regarding variations in mechanical properties during these experiments. Minor differences in material performance were related to the relative hardness of the tempered welds, as well as HAZ softening for the higher strength variants.

6.0 References

(1) Chuko, W. and Gould, J., "Development of Appropriate Resistance Spot Welding Practice for Transformation-Hardened Steels – Phase 2: Evaluation of Post-Weld Cooling Rate Techniques," EWI Report 43280GTH submitted to American Iron and Steel Institute, EWI, Columbus, OH (May 8, 2002).

(2) Peterson, W. and Gould, J., "Development of Appropriate Resistance Spot Welding Practice for Advanced High-Strength Steels – Final Report for Phases 1 and 2," EWI Report 45973GTH submitted to American Iron and Steel Institute, EWI, Columbus, OH (Oct. 9, 2003).

(3) Ford Motor Company, "Resistance Spot Weldability Tests for High Strength Steels," Ford Laboratory Test Methods, BA 13-04 (1980).

(4) "Recommended Practices for Resistance Welding," AWS C1.1-2000, American Welding Society, Miami, FL (Jan. 31, 2000).

(5) "Recommended Practices for Test Methods for Evaluating the Resistance Spot Welding Behavior of Automotive Sheet Steel Materials," AWS/SAE D8.9M:2002, American Welding Society, Miami, FL (April 3, 2002).

(6) Lehman, L. R. and Gould, J. E., "A Study of Resistance Spot Welding Manufacturability Using Design of Experiments, *IBEC 94 Proceedings, Advanced Technologies and Processes*, IBEC Ltd., Warren, MI, pp. 154-163 (1994).

(7) Lehman, L. R. and Gould, J. E., "A Design of Experiments Evaluation of Resistance Spot Welding Manufacturability - Part 2: Multiple Factor Effects," *IBEC 95 Proceedings, Advanced Technologies and Processes*, IBEC Ltd., Warren, MI, pp. 89-99 (1995).

(8) Lehman, L. R. and Gould, J. E., “A Design of Experiments Evaluation of Resistance Spot Welding Manufacturability - Part 3: Optimization and Process Robustness Studies,” *IBEC 96 Proceedings, Advanced Technologies and Processes*, IBEC Ltd., Warren, MI (1996).

(9) Lehman, L., “Operating Procedures for Conducting the A/SP DOE of Coated Steels,” EWI Report 40900CSP submitted to Auto/Steel Partnership, EWI, Columbus, OH (1999).

(10) Gould, J. E., Kimchi, M. and Mitchell, T., “Effect of Fit-Up Conditions when Using Constant Current Control Systems for Resistance Spot Welding,” SAE Technical Paper No. 930451, SAE, Warrendale, PA (1993).

(11) Heuschkel, H. J., "Selecting Spot Welding Schedules for Low Carbon Steels," *Welding Journal Research Supplement*, 25(10):700s-728s (1946).

(12) Nippes, E. F. and Underhill, R. F., "Spot Welding of Heavy Gauge Structural Steel, *Welding Journal Research Supplement*, 28(10):507s-520s (1949).

(13) Gould, J. E. and Lehman, L. R., “A Design of Experiments Evaluation of Factors Affecting the Resistance Spot Weldability of High-Strength Steels,” *Sheet Metal Welding Conference VII*, AWS Detroit Section, Detroit, MI (1996).

(14) Gould, J. E. and Workman, D., “Fracture Morphologies of Resistance Spot Welds Exhibiting Hold Time Sensitivity Behavior,” *Sheet Metal Welding Conference VIII*, AWS Detroit Section, Detroit, MI (1998).

(15) Gould, J. and Peterson, W., “Resistance Welding Research of Coated Steel, Part 6: Electrode Life Studies,” EWI Report J7043-88-6 submitted to AISI, EWI Columbus, OH (1988).

(16) Gould, J. E., “Optimization of a New Resistance Spot Weldability Test for Coated Sheet Steels,” *Sheet Metal Welding Conference IV*, AWS Detroit Section, Detroit, MI (1990).

(17) Peterson, W. and Gould, J., “Development of Spike Temper Diagrams for a Range of Advanced High-Strength Steels,” *Sheet Metal Welding Conference XI*, AWS Detroit Section, Detroit, MI (2004).

(18) Gould, J. E., “An Examination of Nugget Development During Spot Welding Using Both Experimental and Analytical Techniques,” *Welding Journal Research Supplement*, 67(1):1s-10s (1987).

Table 1. Chemistries for the Three Materials

Element	DP600	DP980	M1300
Carbon	0.07	0.14	0.18
Manganese	1.94	1.59	0.40
Phosphorus	0.019	0.018	0.012
Sulfur	0.003	0.004	0.007
Silicon	0.02	0.30	0.20
Chromium	0.15	0.03	0.03
Nickel	0.02	0.02	<0.01
Molybdenum	0.18	<0.01	<0.01
Niobium	0.003	0.002	0.002
Aluminum	0.045	0.043	0.061
Copper	0.03	0.04	0.01
Vanadium	0.004	0.002	0.004
Titanium	0.003	0.005	0.036
Iron	97.5	97.8	99.0

Table 2. DOE Trial Matrix

Trial No.	Quench Time (cycles)	Temper Time (cycles)	BS (vt)	EFD (mm)	Angular Misalignment	Edge Weld	Fitup
1	20	4	4	8	10-degree offset	0.5-mm from edge	2t gap
2	40	4	4	8	Perpendicular	0.5-mm from edge	No gap
3	20	2	4	8	Perpendicular	Center	2t gap
4	40	2	4	8	10-degree offset	Center	No gap
5	20	4	6	8	Perpendicular	Center	No gap
6	40	4	6	8	10-degree offset	Center	2t gap
7	20	2	6	8	10-degree offset	0.5-mm from edge	No gap
8	40	2	6	8	Perpendicular	0.5-mm from edge	2t gap
9	20	4	4	9	10-degree offset	Center	No gap
10	40	4	4	9	Perpendicular	Center	2t gap
11	20	2	4	9	Perpendicular	0.5-mm from edge	No gap
12	40	2	4	9	10-degree offset	0.5-mm from edge	2t gap
13	20	4	6	9	Perpendicular	0.5-mm from edge	2t gap
14	40	4	6	9	10-degree offset	0.5-mm from edge	No gap
15	20	2	6	9	10-degree offset	Center	2t gap
16	40	2	6	9	Perpendicular	Center	No gap

Table 3. Weld and Temper Currents for the Three Materials

Trial No.	DP600 Weld and Temper Currents Force = 5.5 kN Weld Time = 19 cycles				DP980 Weld and Temper Currents Force = 5.5 kN Weld Time = 17 cycles				M1300 Weld and Temper Currents Force = 5.5 kN Weld Time = 17 cycles			
	Weld Current (kA)	Weld Heat (%)	Temper Current (kA)	Temper Heat (%)	Weld Current (kA)	Weld Heat (%)	Temper Current (kA)	Temper Heat (%)	Weld Current (kA)	Weld Heat (%)	Temper Current (kA)	Temper Heat (%)
1	9.0	21	14.7	44	8.4	17	11	22	9.1	20	13.3	32
2	8.0	16	14.7	44	6.1	12	11	22	7.7	15	13.3	32
3	8.0	16	20.6	78	6.1	12	19.8	39	7.7	15	16.9	48
4	9.0	21	20.6	78	8.4	17	19.8	39	9.1	20	16.9	48
5	8.7	20	14.7	44	8.4	19	11	22	9.4	21	13.3	32
6	9.7	24	14.7	44	10.5	26	11	22	11.3	30	13.3	32
7	9.7	24	20.6	78	10.5	26	19.8	39	11.3	30	16.9	48
8	8.7	20	20.6	78	8.4	19	19.8	39	9.4	21	16.9	48
9	10.2	28	14.7	44	9.9	23	11	22	9.7	22	13.3	32
10	9.0	20	14.7	44	7.9	15	11	22	8.2	16	13.3	32
11	9.0	20	20.6	78	7.9	15	19.8	39	8.2	16	16.9	48
12	10.2	28	20.6	78	9.9	23	19.8	39	9.7	22	16.9	48
13	9.6	24	14.7	44	9.5	20	11	22	9.3	21	13.3	32
14	11.9	32	14.7	44	11.2	29	11	22	11.5	30	13.3	32
15	11.9	32	20.6	78	11.2	29	19.8	39	11.5	30	16.9	48
16	9.6	24	20.6	78	9.5	20	19.8	39	9.3	21	16.9	48

Table 4. Raw Static Tensile Data

Trial	DP600 Static Tensile (kN)		DP980 Static Tensile (kN)		M1300 Static Tensile (kN)	
	Replicate 1	Replicate 2	Replicate 1	Replicate 2	Replicate 1	Replicate 2
1	6.85	7.21	8.81	6.54	14.41	16.19
2	7.65	12.37	11.12	12.50	15.75	12.86
3	7.78	12.94	7.70	6.01	9.39	12.14
4	9.03	9.07	14.81	10.68	11.65	14.46
5	20.91	20.19	26.07	24.78	25.00	24.69
6	20.24	19.75	23.04	24.47	29.54	25.84
7	4.36	5.96	19.53	18.82	18.28	20.64
8	16.06	15.39	20.15	20.77	25.67	23.49
9	5.83	5.38	15.08	9.61	12.19	10.45
10	0.00	0.00	0.00	0.00	12.72	11.74
11	4.76	8.67	2.00	5.60	12.72	12.46
12	7.12	7.83	13.79	10.81	4.89	8.63
13	19.08	18.73	10.63	12.10	10.50	11.30
14	12.05	12.01	14.77	14.01	20.60	18.68
15	9.65	6.89	18.46	17.57	27.49	20.37
16	16.10	15.92	19.57	20.33	19.53	24.91

Table 5. Raw Dynamic Tensile Data

	DP600 Impact Energy (J)		DP980 Impact Energy (J)		M1300 Impact Energy (J)	
Trial	Replicate 1	Replicate 2	Replicate 1	Replicate 2	Replicate 1	Replicate 2
1	1.55	3.84	48.1	45.0	25.5	45.0
2	1.25	0.00	0.69	0.72	0.09	9.58
3	41.9	49.2	0.00	0.00	11.9	0.48
4	32.7	40.3	9.13	5.59	11.3	10.7
5	100	143.6	97.0	73.9	78.4	86.7
6	224.5	299	83.0	96.3	90.9	83.2
7	11.7	11.8	34.1	38.4	30.3	56.0
8	52.3	48.6	15.9	24.1	38.3	53.1
9	0.06	67.7	0.03	0.57	8.26	16.6
10	0.00	0.00	0.00	0.00	18.2	16.0
11	0.19	0.48	0.12	0.00	13.2	1.74
12	23.6	33.2	32.9	49.7	9.22	0.55
13	128.3	113.9	4.70	23.7	22.4	45.3
14	62.0	92.5	50.7	65.7	31.1	55.0
15	150.6	61.8	47.9	33.8	23.8	26.3
16	86.0	67.1	51.2	42.0	68.2	58.0

Table 6. Normalization Functions and Related Correlation Coefficients for Each of the Response Factors Examined in this Study

Response Factor	Normalization Function	Correlation Factor (%)
DP600 Static Tensile	None	97.7
DP980 Static Tensile	None	99.3
DP1300 Static Tensile	None	97.5
DP600 Dynamic Tensile	X(600Dt) = sinh(600Dt-165/75)	98
DP980 Dynamic Tensile	None	96
DP1300 Dynamic Tensile	X(1300Dt) = sinh(1300Dt-160/75)	99

Table 7. Regression Analysis Results for the DP600 Peak Load

Regression Equation:				
Pk Load-600 = 2428 - 216 TempTime + 848 BS - 321 EFD + 332 AngularMis + 391 QT*TT + 198 QT*BS - 220 QT*EFD - 524 EFD*Edge + 146 TT*Edge + 270 TT*EFD + 108 QuenchTime - 100 QT*Edge + 96 EdgeWeld				
Predictor	**Coef**	**SE Coef**	**T**	**P**
Constant	2428	75.01	32.37	0.000
TempTime	-216	75.01	-2.87	0.010
BS	848	75.01	11.31	0.000
EFD	-321	75.01	-4.28	0.000
AngularM	332	75.01	4.43	0.000
QT*TT	391	75.01	5.21	0.000
QT*BS	198	75.01	2.64	0.017
QT*EFD	-220	75.01	-2.93	0.009
EFD*Edge	-524	75.01	-6.98	0.000
TT*Edge	146	75.01	1.94	0.068
TT*EFD	270	75.01	3.61	0.002
QuenchTi	108	75.01	1.44	0.166
QT*Edge	-100	75.01	-1.34	0.198
EdgeWeld	96	75.01	1.29	0.215
S = 424.3	R-Sq = 94.1%	R-Sq(adj) = 89.9%		

Table 8. Regression Analysis Results for the DP980 Peak Load

Predictor	Coef	SE Coef	T	P
Regression Equation:				
Pk Load-980 = 3092 + 151 QuenchTime + 1194 BS - 502 EFD - 291 AngularMis + 254 EdgeWeld + 270 Fitup + 344 QT*TT - 325 QT*Edge - 203 TT*Edge + 357 TT*EFD - 120 AA*EDGE				
Constant	3092	78.46	39.41	0.000
QuenchTi	151	78.46	1.92	0.069
BS	1194	78.46	15.22	0.000
EFD	-502	78.46	-6.40	0.000
AngularM	-291	78.46	-3.70	0.001
EdgeWeld	254	78.46	3.23	0.004
Fitup	270	78.46	3.44	0.003
QT*TT	344	78.46	4.38	0.000
QT*Edge	-325	78.46	-4.15	0.000
TT*Edge	-203	78.46	-2.59	0.018
TT*EFD	357	78.46	4.55	0.000
AA*EDGE	-120	78.46	-1.54	0.140
S = 443.8		R-Sq = 95.0%		R-Sq(adj) = 92.2%

Table 9. Regression Analysis Results for the M1300 Peak Load

Predictor	Coef	SE Coef	T	P
Regression Equation:				
Pk Load-1300_1 = 3788 + 1081 BS - 427 EFD + 317 EdgeWeld - 164 QT*TT + 261 QT*BS + 241 EFD*Edge + 361 TT*EFD				
Constant	3788	109.7	34.52	0.000
BS	1081	109.7	9.85	0.000
EFD	-427	109.7	-3.90	0.001
EdgeWeld	317	109.7	2.88	0.008
QT*TT	-164	109.7	-1.49	0.149
QT*BS	261	109.7	2.38	0.026
EFD*Edge	241	109.7	2.19	0.038
TT*EFD	361	109.7	3.29	0.003
S = 620.7		R-Sq = 85.7%	R-Sq(adj) = 81.6%	

Table 10. Regression Analysis Results for the DP600 Impact Energy (Analysis is based on normalized data transformed using the equation given in Table 6.)

Regression Equation:				
X_600_Impact = - 5.08 + 2.32 BS + 1.23 EdgeWeld - 0.681 Fitup - 0.427 QT*EFD - 1.35 EFD*Edge + 0.429 QT*TT - 0.288 TempTime + 0.368 QT*BS - 0.347 AngularMis				
Predictor	**Coef**	**SE Coef**	**T**	**P**
Constant	-5.08	0.2389	-21.25	0.000
BS	2.32	0.2389	9.70	0.000
EdgeWeld	1.23	0.2389	5.15	0.000
Fitup	-0.681	0.2389	-2.85	0.010
QT*EFD	-0.427	0.2389	-1.79	0.089
EFD*Edge	-1.35	0.2389	-5.65	0.000
QT*TT	0.429	0.2389	1.79	0.087
TempTime	-0.288	0.2389	-1.21	0.241
QT*BS	0.368	0.2389	1.54	0.139
AngularM	-0.347	0.2389	-1.45	0.161
S = 1.322		R-Sq = 88.4%	R-Sq(adj) = 83.4%	

Table 11. Regression Analysis Results for the DP980 Impact Energy

Regression Equation:				
980_Impact = 30.4 + 2.53 QuenchTime - 6.43 TempTime + 18.4 BS - 5.29 EFD - 9.60 AngularMis + 3.33 EdgeWeld + 2.27 QT*TT + 2.19 QT*BS + 8.84 AA*Edge - 6.55 EFD*Edge - 3.64 TT*Edge + 13.4 BS*Edge				
Predictor	**Coef**	**SE Coef**	**T**	**P**
Constant	30.4	1.443	21.10	0.000
QuenchTi	2.53	1.443	1.75	0.096
TempTime	-6.43	1.443	-4.46	0.000
BS	18.4	1.443	12.79	0.000
EFD	-5.29	1.443	-3.67	0.002
AngularM	-9.60	1.443	-6.65	0.000
EdgeWeld	3.33	1.443	2.31	0.033
QT*TT	2.27	1.443	1.57	0.133
QT*BS	2.19	1.443	1.52	0.146
AA*Edge	8.84	1.443	6.13	0.000
EFD*Edge	-6.55	1.443	-4.54	0.000
TT*Edge	-3.64	1.443	-2.52	0.021
BS*Edge	13.4	1.443	9.30	0.000
S = 7.955		R-Sq = 95.8%		R-Sq(adj) = 93.0%

Table 12. Regression Analysis Results for the M1300 Impact Energy (Analysis is based on normalized data transformed using the equation given in Table 6.)

Regression Equation:				
X_1300 = - 1.92 + 1.91 BS - 0.509 EFD + 0.439 EdgeWeld + 0.405 QT*BS + 0.347 QT*EFD + 0.008 EFD*Edge				
Predictor	**Coef**	**SE Coef**	**T**	**P**
Constant	-1.92	0.2528	-7.75	0.000
BS	1.91	0.2528	7.69	0.000
EFD	-0.509	0.2528	-2.05	0.050
EdgeWeld	0.439	0.2528	1.77	0.088
QT*BS	0.405	0.2528	1.63	0.114
QT*EFD	0.347	0.2528	1.40	0.173
S = 1.402	R-Sq = 73.2%	R-Sq(adj) = 68.1%		

Table 13. Nugget and Button Measurements from Processed Static Tensile Coupons

	DP600		**DP980**		**M1300**	
Run	**Average Nugget Dia. (mm)**	**Average Button Dia. (mm)**	**Average Nugget Dia. (mm)**	**Average Button Dia. (mm)**	**Average Nugget Dia. (mm)**	**Average Button Dia. (mm)**
1	4.63		3.40		4.66	
2	4.76		4.50		4.87	
3	5.63		3.82		4.45	
4	4.80		4.55		4.90	
5	6.36		6.30		6.10	
6	6.8		6.34		7.04	
7	6.0	3.73	5.13			6.24
8	7.5			6.44	6.72	
9	3.80		4.49		3.91	
10	N/A		N/A		4.38	
11	5.19		6.11		5.06	
12	4.33		4.66		3.23	
13		9.70		4.26	7.02	
14	6.80	4.00	4.63			7.47
15	7.01		5.95		6.86	
16	6.15		5.63		5.99	

Table 14. Nugget and Button Measurements from Processed Dynamic Tensile Coupons

Run	DP600		DP980		M1300	
	Average Nugget Dia. (mm)	Average Button Dia. (mm)	Average Nugget Dia. (mm)	Average Button Dia. (mm)	Average Nugget Dia. (mm)	Average Button Dia. (mm)
1	6.015			4.66		5.595
2	5.2		5.335		6.415	
3	5.64		4.535		4.89	
4	5.105		4.71		5.15	
5	8.01		6.625		5.72	
6	6		8.445		7.185	
7	6.415			6.25		6.85
8	6.82		5.035			7.3
9	7.945		5.05		5.045	
10	N/A				4.53	
11	5.255		3.75		4.95	
12	4.78			4.99	4.715	
13		8.065	4.75		7.25	
14	6.71			6.43		6.63
15	6.705		7.89		8	
16	6.685		5.825		6.475	

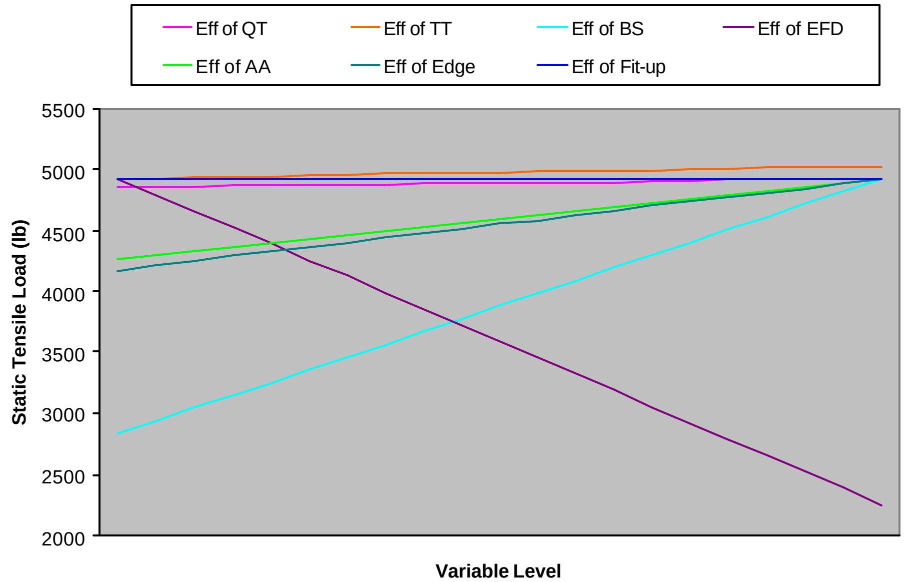

Quench Time	20 cycles <---> 40 cycles
Temper Time	4 cycles <---> 2 cycles
Button Size	4 root T <---> 6 root T
Electrode Face	8 mm <---> 9 mm
Angular Miss-Align	10 deg <---> None
Weld Position	Edge <---> Center
Fit-up	2T Gap <---> No Gap

Figure 1. Process Robustness Plot Showing the Effects of Process Conditions on DP600 Static Tensile Shear Results (The plot is anchored on a set of base conditions that include 40-cycle quench time, 4-cycle temper time, 6vt button size, 8-mm electrode diameter, perpendicular angular alignment, a center weld location, and good fitup.)

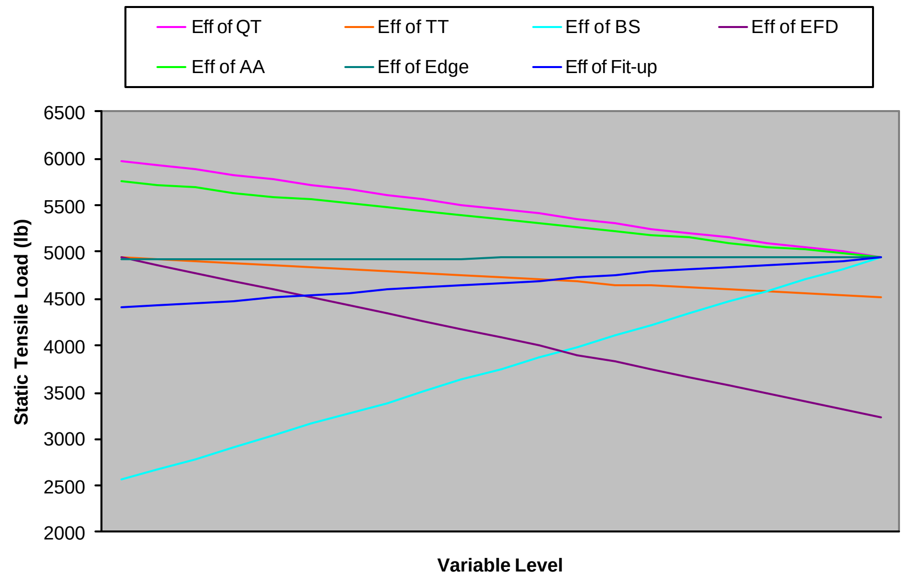

Quench Time	20 cycles <--->	40 cycles
Temper Time	4 cycles <--->	2 cycles
Button Size	4 root T <--->	6 root T
Electrode Face	8 mm <--->	9 mm
Angular Miss-Align	10 deg <--->	None
Weld Position	Edge <--->	Center
Fit-up	2 T Gap <--->	No Gap

Figure 2. Process Robustness Plot Showing the Effects of Process Conditions on DP980 Static Tensile Shear Results (The plot is anchored on a set of base conditions that include 40-cycle quench time, 4-cycle temper time, 6vt button size, 8-mm electrode diameter, perpendicular angular alignment, a center weld location, and good fitup.)

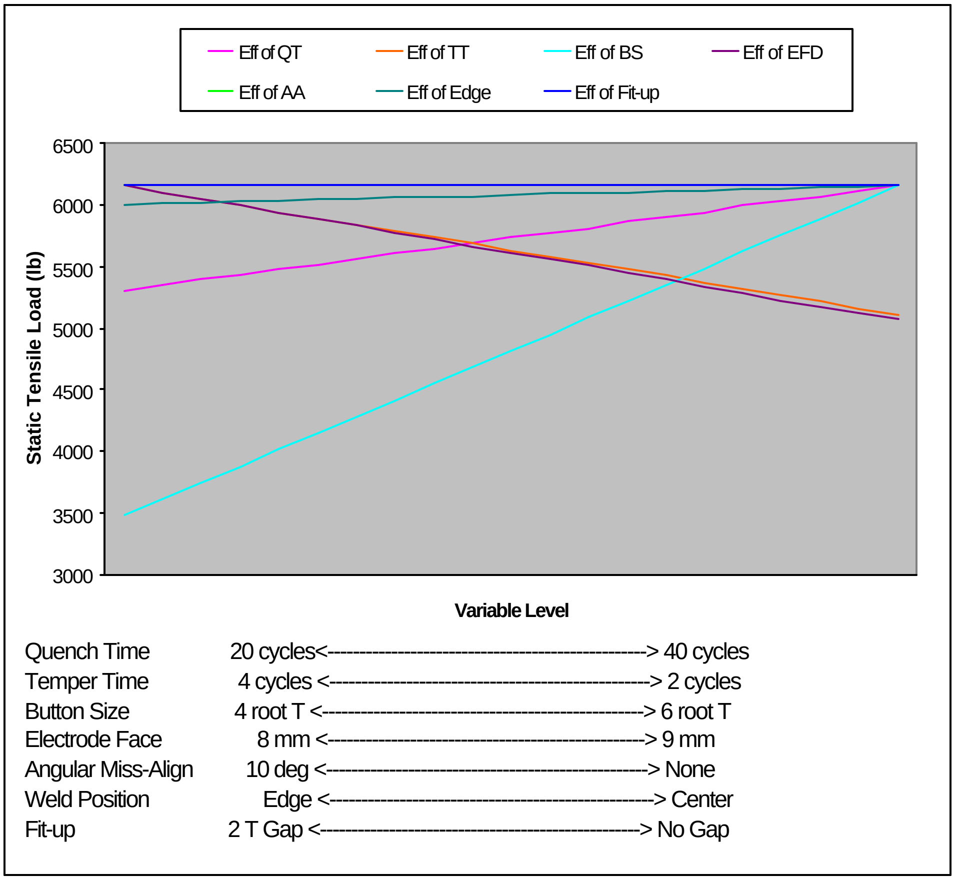

Figure 3. Process Robustness Plot Showing the Effects of Process Conditions on M1300 Static Tensile Shear Results (The plot is anchored on a set of base conditions that include 40-cycle quench time, 4-cycle temper time, 6vt button size, 8-mm electrode diameter, perpendicular angular alignment, a center weld location, and good fitup.)

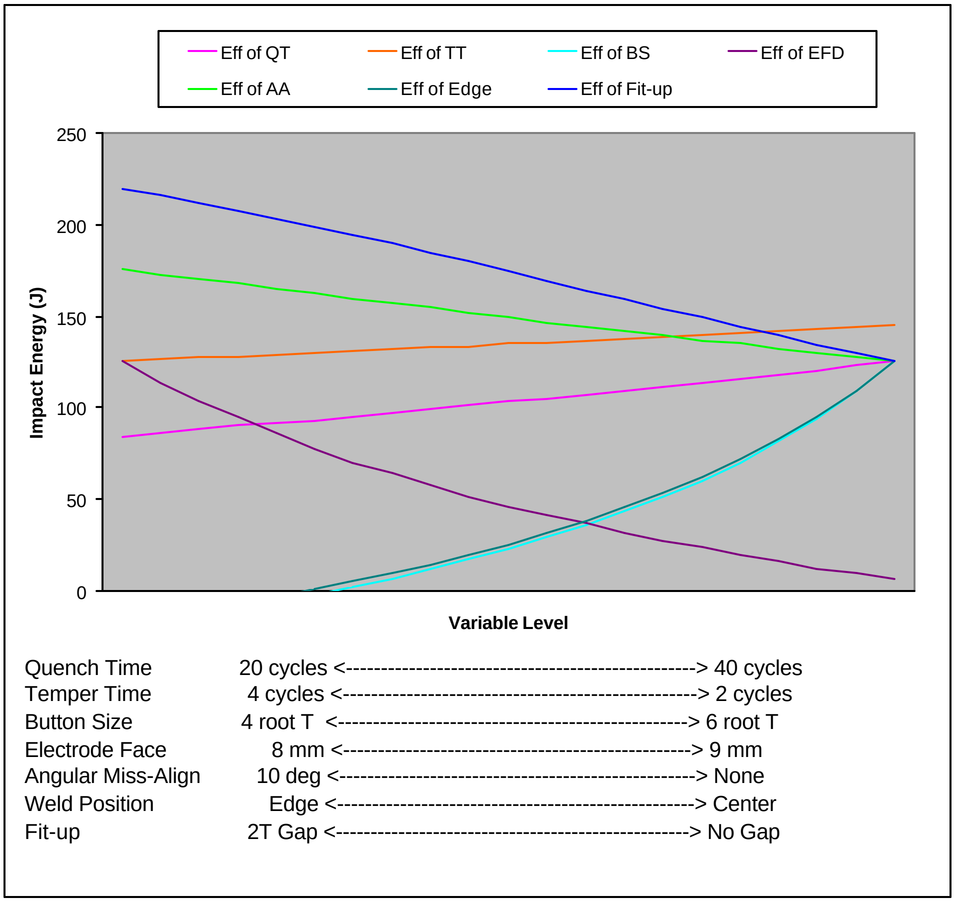

Figure 4. Process Robustness Plot Showing the Effects of Process Conditions on DP600 Dynamic Tensile Shear Results (The plot is anchored on a set of base conditions that include 40-cycle quench time, 4-cycle temper time, 6vt button size, 8-mm electrode diameter, perpendicular angular alignment, a center weld location, and good fitup.)

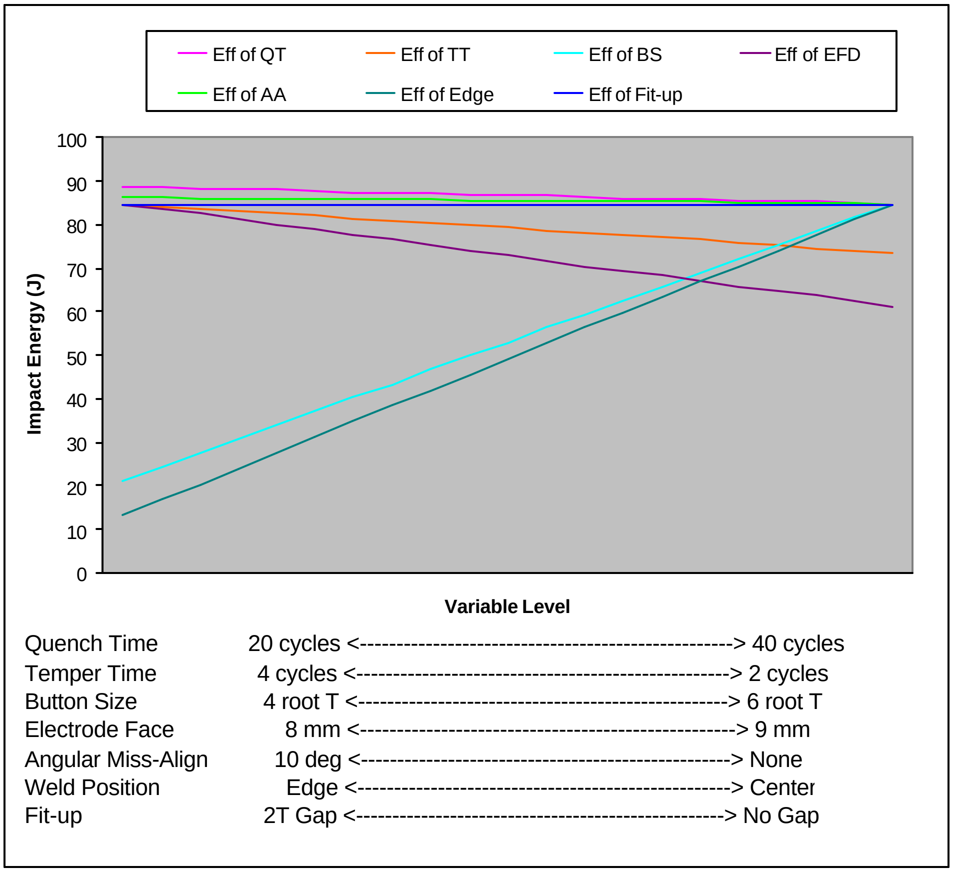

Figure 5. Process Robustness Plot Showing the Effects of Process Conditions on DP980 Dynamic Tensile Shear Results (The plot is anchored on a set of base conditions that include 40-cycle quench time, 4-cycle temper time, 6vt button size, 8-mm electrode diameter, perpendicular angular alignment, a center weld location, and good fitup.)

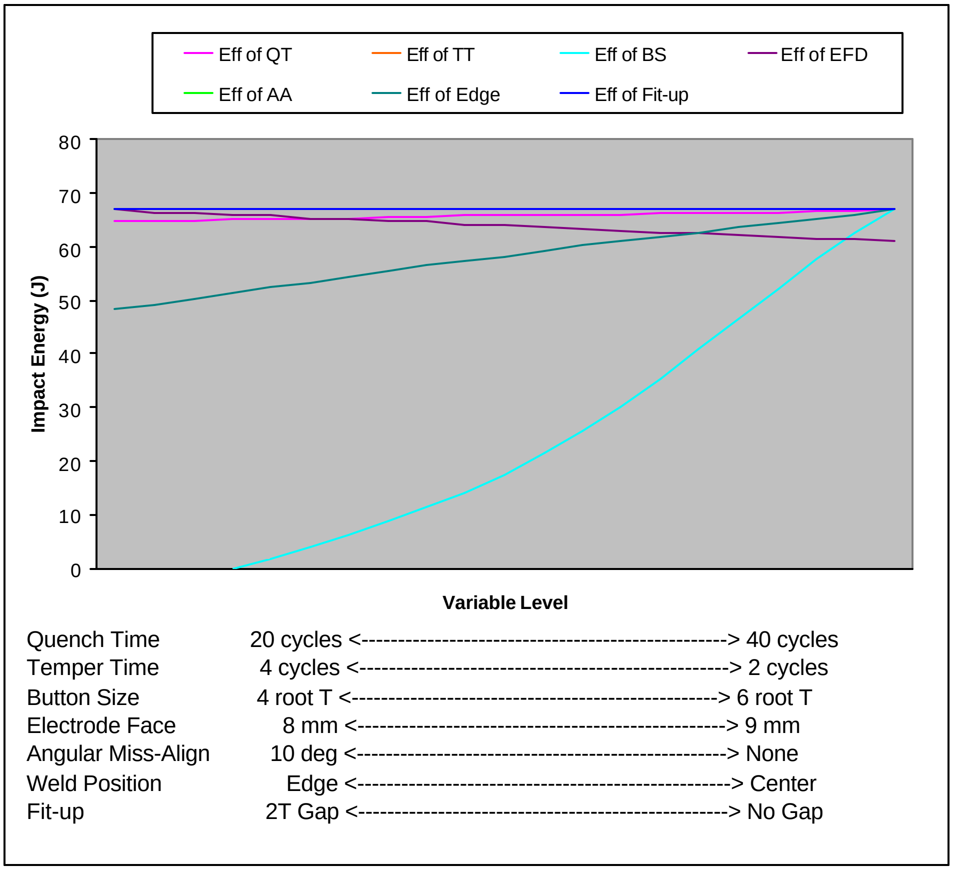

Figure 6. Process Robustness Plot Showing the Effects of Process Conditions on M1300 Dynamic Tensile Shear Results (The plot is anchored on a set of base conditions that include 40-cycle quench time, 4-cycle temper time, 6vt button size, 8-mm electrode diameter, perpendicular angular alignment, a center weld location, and good fitup.)

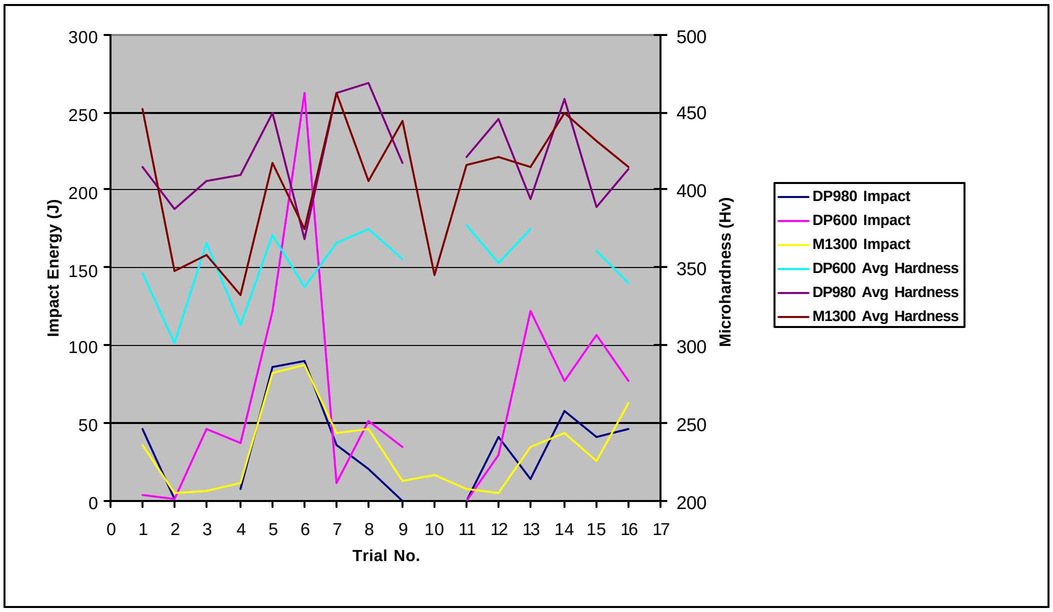

Figure 7. Correlations between Impact Energy and Average Microhardness by Trial Number

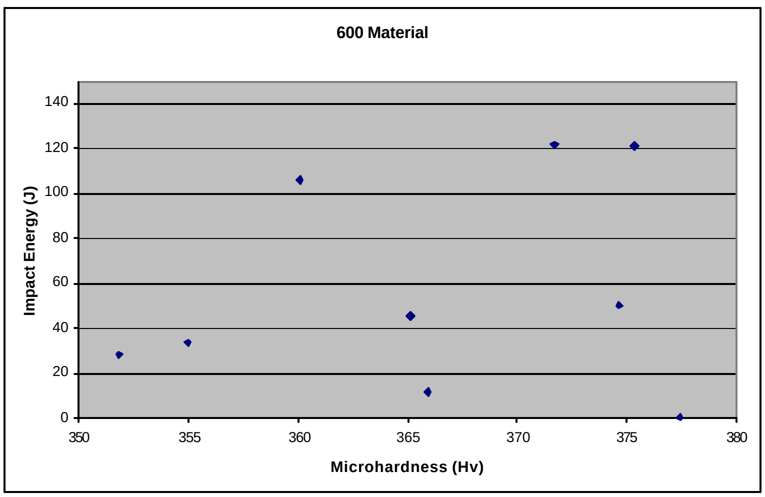

Figure 8. Correlations between Impact Energy and Average Microhardness for DP600

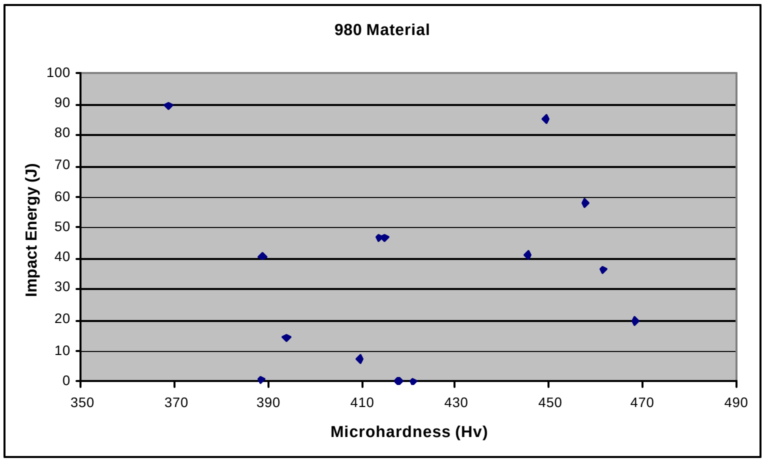

Figure 9. **Correlations between Impact Energy and Average Microhardness for DP980**

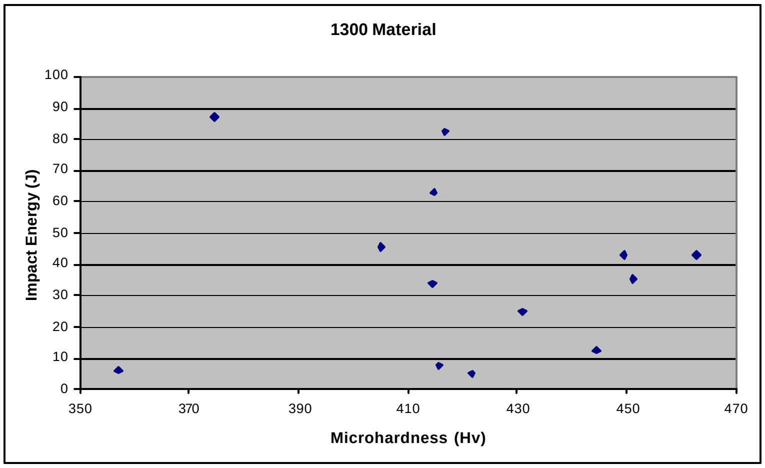

Figure 10. **Correlations between Impact Energy and Average Microhardness for M1300**